



Contents lists available at ScienceDirect

Arabian Journal of Chemistry

journal homepage: www.sciencedirect.com

Original article

Facile fabrication of hollow molecularly imprinted polymer microspheres via pickering emulsion polymerization stabilized with TiO₂ nanoparticles



Zehu Wang^{a,b,c,*}, Zongqi Li^{a,b,c}, Ruiye Yan^{d,*}, Guangshuo Wang^{a,b,c}, Yanming Wang^{a,b,c}, Xiaoliang Zhang^{a,b,c}, Zhixiao Zhang^{a,b,c}

^a College of Materials Science and Engineering, Hebei University of Engineering, Handan 056038, PR China

^b Technology Innovation Center of Modified Plastics of Hebei Province, Handan 056038, PR China

^c Key Laboratory of New Inorganic Nonmetallic Composite Materials of Handan, Handan 056038, PR China

^d Academic Affairs Office, Hebei University of Engineering, Handan 056038, PR China

ARTICLE INFO

Article history:

Received 10 May 2023

Accepted 21 September 2023

Available online 26 September 2023

Keywords:

Hollow structure

Molecularly imprinted polymers

Pickering emulsion polymerization

TiO₂ nanoparticles

Dibutyl phthalate

ABSTRACT

The polymer microspheres with hollow structure are of technological importance in the removal of pollutants because of the large specific surface area and low mass transfer resistance. In this work, we employ the Pickering emulsion polymerization stabilized with TiO₂ nanoparticles to build the molecularly imprinted polymers microspheres with hollow structure (H-MIPs) for the precise recognition of dibutyl phthalate (DBP), which would influence the biological reproductive system and endocrine system as a typical endocrine disrupting compound. The polymerization induced phase separation occurring within Pickering emulsion droplets plays a significant role in the formation of hollow structure. The morphology and structure of H-MIPs were observed via optical microscope and field emission scanning electron microscope, respectively. The results indicate that H-MIPs microspheres are of irregular spherical form with sunken surface and perfect hollow structure. The forming process of the hollow structure was analyzed in detail. Besides, the chemical structure and thermal stability of H-MIPs and H-NIPs were characterized by fourier transform infrared spectroscopy and thermal gravimetric analysis, respectively. The binding performance of H-MIPs and H-NIPs was investigated through a series of binding experiments, which consist of the binding kinetics, binding isotherm, selective test and reusability experiment. The results show that H-MIPs microspheres exhibit remarkable binding kinetics towards DBP, and the saturated adsorption time is not more than 30 min. Apart from the fast binding rate, H-MIPs also show considerable binding amount, accurate binding selectivity and good regenerability. The imprinting factor could reach to 2.56, and the binding amount towards DBP remains at a relatively high level within 3 cycles. The prepared H-MIPs microspheres have broad application prospects in environmental and analytical field involved DBP, and the study also offers an alternative method for the facile building of H-MIPs microspheres.

© 2023 The Author(s). Published by Elsevier B.V. on behalf of King Saud University. This is an open access article under the CC BY-NC-ND license (<http://creativecommons.org/licenses/by-nc-nd/4.0/>).

1. Introduction

As a kind of plasticizers, phthalic acid esters are used widely in plastic industry. The addition of phthalic acid esters could significantly

improve the flexibility and durability of plastic products (Mahajan et al., 2019). However, there are no chemical bonds formed between plastic matrix and phthalic acid esters, so the phthalic acid esters are easy to dissolve out from plastic products and diffuse into the environments as time passes (Gao et al., 2016). As endocrine disrupting compounds, the phthalic acid esters present in the environment would influence the biological reproductive system and endocrine system. Besides, the phthalic acid esters could also cause deformity, cancer and gene mutations of the biological body even at very low concentration because of their easy migration and enrichment in organism (Tian et al., 2020). Therefore, the effective separation and analysis of phthalic acid esters in environmental samples becomes extremely important.

* Corresponding authors.

E-mail addresses: wangzehu12@126.com (Z. Wang), 253041131@qq.com (R. Yan).

Peer review under responsibility of King Saud University.



Production and hosting by Elsevier

<https://doi.org/10.1016/j.arabjc.2023.105304>

1878-5352/© 2023 The Author(s). Published by Elsevier B.V. on behalf of King Saud University.

This is an open access article under the CC BY-NC-ND license (<http://creativecommons.org/licenses/by-nc-nd/4.0/>).

However, the phthalic acid esters often coexist with other chemical substances in very low concentration (Nguyen et al., 2019). Due to the lack of selectivity, the traditional adsorption materials are limited to some degree in use (Jena et al., 2021; Htwe et al., 2022). Thus, the development of new materials with high selectivity towards phthalic acid esters is urgent. Scheme 1.

Molecular imprinting technology provides us with a powerful tool to prepare molecularly imprinted polymers (MIPs) with specific molecular recognition sites (Wang et al., 2018). MIPs have a predetermined selectivity towards the target molecules because of their participation in the preparation process. The highly cross-linked structure of MIPs could maintain the characters of microcavities when the target molecules are removed, which are complementary with target molecules in both shape and chemical functionality (He et al., 2021). Therefore, the MIPs could be used to absorb selectively the target molecules in the separation or analysis process. Numerous studies have shown that MIPs are of excellent selectivity (BelBruno et al., 2019). The MIPs are often prepared by bulk polymerization because of its simple experimental device, easy operation control and high universality. However, the bulk polymerization also faces some challenges. MIPs prepared by bulk polymerization are usually bulk materials, which need to subject the laborious pretreatment procedure, which includes crushing, grinding and screening before use. Besides, some imprinted sites would be destroyed during the crushing process, which would lead to a decrease in the utilization rate of imprinted sites. Furthermore, the MIPs particles obtained by screening are irregular in shape and uneven in size, which would exert negative influence on the application (Wulff et al., 2013).

Due to the limitations of bulk polymerization, the preparing methods of MIPs with preordered form have been developed, which include suspension polymerization (Liu et al., 2019), precipitation polymerization (Min et al., 2021), emulsion polymerization (Wang et al., 2018), swelling polymerization (Kubo et al., 2021), sol-gel method (Luo et al., 2022) and so on. These methods could prepare spherical MIPs microspheres. Therefore, the laborious pretreatment procedure, such as crushing, grinding and screening, could be omitted before use. Even so, the embedding of imprinting sites still exists for these MIPs microspheres, which have no essential difference with the products prepared by bulk polymerization apart from the product form. The limitations of products prepared by bulk polymerization, such as poor sites accessibility, template leakage, slow binding kinetics and low binding amount, still have not been solved effectively (Bayramoglu et al., 2016).

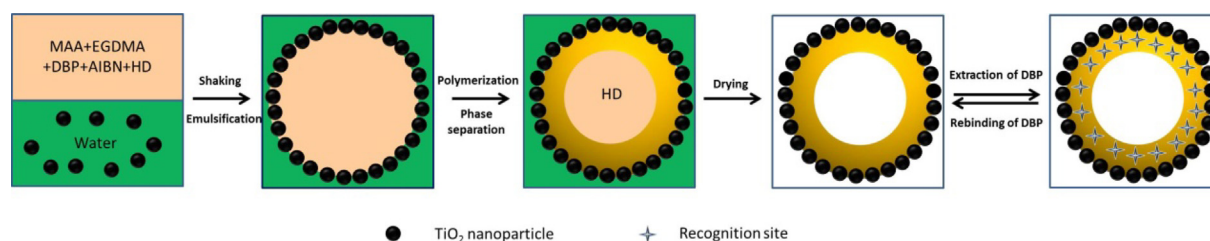
Based on the above problems, the surface molecular imprinting technology is proposed, which could solve effectively the embedding of imprinted sites. A thin MIPs layer could be grafted or coated on the surface of the substrate material by surface molecular imprinting technology, which makes the imprinted sites accessible (Karsten et al., 2020). MIPs prepared by surface molecular imprinting technology are referred to as surface MIPs (S-MIPs). Compared with traditional MIPs, S-MIPs have many advantages. Firstly, the removal and rebinding of template molecules become much easier because of the presence of thin MIPs layer. Secondly, the appear-

ance of S-MIPs depends on the used substrate material, so it could be designed as needed (Guo et al., 2018). Although S-MIPs have remarkable advantages in improving the utilization of imprinting sites, they still face some limitations. Firstly, the binding amount would be influenced to some extent because of the presence of substrate material, on which the imprinted sites are absent. Besides, the surface of substrate material often needs tedious treatment before the coating or grafting of MIPs layer (Zhang et al., 2020).

In recent years, the design and preparation of hollow microspheres have gained wide attention because of their lower density and larger cavity volume. The hollow microspheres have potential application prospect in controlled drug release, separation of environmental pollutants and catalytic reactors (Pan et al., 2014). For MIPs microspheres, the introduction of hollow structure could increase their binding amount and accelerate binding rate because of the large surface area and absence of support materials, which are both beneficial to for mass transfer (Zhang et al., 2019). The hollow MIPs (H-MIPs) microspheres are usually prepared by surface imprinting technology combined with the following calcination or dissolution, which could remove the substrate material effectively (Xu et al., 2011). In the preparation process, the substrate material is essential, which usually serve as sacrificial cores and need to be removed in the post-treatment procedure. The extra post-treatment is laborious. Besides, the high temperature required for calcination and the use of organic solvents in etching are both environmentally unfriendly and would inevitably lead to higher cost (Mokhtari et al., 2019). Therefore, the facile methods for preparing H-MIPs are urgently needed. However, the relevant reports are still scarce.

Pickering emulsions are usually stabilized by colloid solid particles rather than surfactants (Pickering 1907). In many cases, the stability of Pickering emulsions is much higher than conventional emulsions stabilized by surfactants. Besides, the colloidal solid particles are much more environmentally friendly compared with the surfactants. Recently, Pickering emulsion polymerization has attracted great enthusiasm as a powerful technique for the fabrication of functional materials with well-designed structures. Numerous researches indicate that Pickering emulsions could provide an alternative platform for the fabrication of complex micro- and nanostructures (Shen et al., 2011). Moreover, it has been widely accepted that the well-designed structure could endow the material with fascinating features (Zhang et al., 2014). Up to now, numerous solid particles, such as silica, laponite clay, magnetite, zinc oxide and graphene oxide, have been successfully used as the Pickering stabilizer to prepare hybrid microspheres or nanoparticles. Except for the inorganic particles, the cross-linked polymer particles could also be employed as stabilizers to generate Pickering emulsions (Schrade et al., 2013).

Recently, TiO₂ nanoparticles have been used continually in both photochemical and photocatalytic fields (Monllorsatoca et al., 2021; Jia et al., 2021; Eidsvg et al., 2021). As a kind of inorganic material, TiO₂ nanoparticles are one of the most promising photocatalyst for their advantageous properties such as nontoxic, low-



Scheme 1. Schematic illustration for the fabrication of H-MIPs microspheres by Pickering emulsion polymerization.

cost, chemical inertness and photostability (Dharma et al., 2022; Sun et al., 2020). TiO₂ nanoparticles are often used as the photocatalytic component for the fabrication of various functional materials (Roberto et al., 2019; Zarhri et al., 2020; Ziat et al., 2022; Belkhanchi et al., 2021; Belkhanchi et al., 2020). However, the photocatalytic oxidation of TiO₂ nanoparticles is not a selective process, which is driven by the formation of hydroxyl radicals. Therefore, the organic compounds present in the environment at high concentration could be efficiently degraded, whereas the organic compounds at low concentration are hard to remove. It is well known that the molecular imprinting is a fascinating and innovative technique to obtain an efficient and selective material in the elimination of recalcitrant pollutants. Therefore, we intend to use TiO₂ nanoparticles as Pickering emulsion stabilizer for the fabrication of H-MIPs microspheres, which would be of rebinding selectivity and photocatalytic activity simultaneously.

In this contribution, we described the building of H-MIPs microspheres via Pickering emulsion polymerization. The polymerization induced phase separation plays an important role in the fabrication of hollow structure. The whole building process of H-MIPs microspheres is shown in Scheme 1. In the preparation process, TiO₂ nanoparticles were used as Pickering emulsion stabilizer because of their suitable hydrophilicity. Dibutyl phthalate (DBP), one of the extensively used phthalic acid esters, was selected as template molecules. Methacrylic acid (MAA) was chosen to serve as the functional monomer, and ethylene glycol dimethacrylate (EGDMA) was used for cross-linker. In addition, the hexadecane, a nonreactive solvent, was also added to the component, which served as phase separation agent of polymerization reaction. The H-MIPs microspheres were observed by optical microscope and field emission scanning electron microscope, respectively. The results indicate that the obtained H-MIPs microspheres are of perfect hollow structure, and their diameter vary from 19 to 100 μm. The forming process of hollow structure was discussed. The chemical structure and thermal stability of H-MIPs microspheres were characterized by fourier transform infrared spectroscopy and thermal gravimetric analysis, respectively. The binding properties of H-MIPs microspheres were investigated systematically, which included the binding kinetics, binding isotherm, selective tests and the reusability. The results indicate that H-MIPs microspheres exhibit remarkable binding kinetics, desirable binding amount and selectivity towards DBP. The excellent specificity provides a bright application prospect for H-MIPs microspheres.

2. Experimental

2.1. Materials

Diamyl phthalate (DAP), Dioctyl phthalate (DOP), Dimethyl phthalate (DMP) and DBP were all purchased from Energy Chemical Company. The initiator azobisisobutyronitrile (AIBN) was obtained from Sinopharm Chemical Reagent Company. The functional monomer MAA was ordered from Aladdin Reagent Company. Hexadecane (HD) and EGDMA were provided by J&K Scientific. TiO₂ nanoparticles were purchased from Degussa (China) Company Limited. Acetic acid and Methanol were both supplied by Oubokai Agent Factory. The water used was ultrapure water.

2.2. Characterization

The morphology and size of Pickering emulsion droplets stabilized with TiO₂ nanoparticles were observed by optical microscope (OLYMPUS SX500). The morphology of TiO₂ nanoparticles was characterized by field emission scanning electron microscope

(FESEM, SU8200, HITACHI). The morphology and size of H-MIPs and H-NIPs microspheres were assessed using OLYMPUS SX500 and FESEM (SU8200, HITACHI), respectively. The size distribution frequency of H-MIPs and H-NIPs microspheres was analyzed by the software of Nano Measurer 1.2. Fourier transform infrared (FTIR) spectra of H-MIPs and H-NIPs microspheres were obtained by infrared spectrometer (FTIR-650, Tianjin Gangdong). Thermal gravimetric analysis (TGA) of H-MIPs and H-NIPs microspheres was conducted using an instrument (TGA, 4000, PerkinElmer) with a heating rate of 10 K/min under nitrogen atmosphere between room temperature and 800 °C. The concentration of DBP, DAP, DMP and DOP in solutions was all determined by ultraviolet–visible spectrophotometer (UV–vis, T6NEW CENTURY, PGENERAL).

2.3. Fabrication of H-MIPs microspheres

In this study, Pickering emulsion polymerization with TiO₂ nanoparticles as the stabilizer was employed for the building of H-MIPs microspheres. Briefly, 20 mg of TiO₂ nanoparticles and 5.0 mL of ultrapure water were added to the standard vessel successively. Then, the standard vessel loaded with TiO₂ nanoparticles and ultrapure water was transferred to the ultrasonic cleaner and subjected to the ultrasonic treatment for 5 min. The obtained suspension liquid was called as water phase. MAA (0.136 mL), EGDMA (0.905 mL), DBP (0.105 mL), HD (1.000 mL) and AIBN (20.0 mg) were mixed and subjected to the magnetic stirring to obtain the homogeneous solution, which was labeled as an oil phase. The Pickering emulsion was obtained by violent shaking for 5 min after the oil phase was mixed with the water phase. The nitrogen gas was pumped into the vessel for 15 min to expel oxygen. After that, the vessel was sealed up and heated through water bath to polymerize for 16 h at 70 °C. The microspheres were collected by filtration when the temperature dropped to room temperature. In order to remove DBP, the microspheres were extracted repeatedly by methanol/acetic acid (90:10, v/v) until DBP could not be detected from the washing solvent by UV–vis. After drying to constant weight, the H-MIPs microspheres were obtained. As a contrast, the hollow non-imprinted polymers (H-NIPs) microspheres were also prepared synchronously using the same procedure, except that no template molecule of DBP was added.

2.4. Binding experiments

The binding experiments consist of the binding kinetics experiment, binding isothermal experiment and binding selectivity experiment. The binding kinetics experiment was performed firstly. Briefly, 20 mg of H-MIPs or H-NIPs were mixed with 10.0 mL of DBP ethanol solution with the concentration of 1.0 mmol/L. The mixtures were incubated for different time at room temperature. H-MIPs or H-NIPs microspheres were separated by means of filtration when the desired time arrived. The residual DBP amount in the solution was monitored by UV–vis. The binding amount of H-MIPs or H-NIPs at the desired time was obtained by the concentration difference of DBP according to the following equation:

$$B_t = (C_0 - C_t) \nu / m \quad (1)$$

where C_0 and C_t are the initial concentration of DBP and the residual concentration at desired time, respectively. ν stands for the volume of the DBP ethanol solution, m is the mass of H-MIPs or H-NIPs microspheres, and B_t is the binding amount of H-MIPs or H-NIPs microspheres at desired time.

The binding isothermal experiment was carried out as follows. 20 mg of H-MIPs or H-NIPs microspheres was separately added to 10.0 mL of DBP ethanol solution with different initial concentrations (0.5–3.0 mmol/L). The mixtures were incubated for 12 h at

room temperature. After reaching equilibrium, the H-MIPs or H-NIPs microspheres were separated by means of filtration. The residual DBP amount in the solution was monitored by UV-vis. The equilibrium binding amount of H-MIPs or H-NIPs was obtained by the concentration difference of DBP using the following equation:

$$B = (C_0 - F)v/m \quad (2)$$

where C_0 and F are the initial and equilibrium concentrations of DBP, respectively. v stands for the volume of DBP ethanol solution, m is the mass of H-MIPs or H-NIPs microspheres, and B is the equilibrium binding amount of H-MIPs or H-NIPs microspheres.

The binding selectivity of H-MIPs or H-NIPs microspheres was evaluated using DBP and its three structural analogs (DAP, DMP and DOP). Briefly, 20 mg of H-MIPs or H-NIPs microspheres was added to the screw bottles, which contained 10.0 mL of ethanol solutions with 1.0 mmol/L of DBP, DAP, DMP and DOP, respectively. The mixtures were incubated for 12 h at room temperature. At the desired time, the H-MIPs or H-NIPs microspheres were separated by means of filtration. The residual amounts of DBP, DAP, DMP and DOP were monitored by UV-vis. The binding amounts of H-MIPs or H-NIPs towards DBP, DAP, DMP and DOP were obtained by the concentration difference using equation (2).

2.5. Reusability experiment

To characterize the stability of H-MIPs and H-NIPs microspheres, the reusability experiment was conducted. Briefly, 20 mg of H-MIPs or H-NIPs microspheres was added to 10.0 mL of DBP ethanol solution with the concentration of 1.0 mmol/L. Then, the mixtures were incubated for 12 h at room temperature. At the desired time, the H-MIPs or H-NIPs microspheres were collected by means of filtration using nylon 66 microporous filter membrane. The UV-vis was used to monitor the residual DBP concentration in the solution. To remove DBP completely, the adsorbed H-MIPs and H-NIPs microspheres were washed thoroughly with the mixed solvent of methanol/acetic acid (90:10, v/v). The regenerative H-MIPs and H-NIPs microspheres were used for the next sorption-desorption cycle. The sorption-desorption cycle was carried out repeatedly for 5 times.

3. Results and discussion

3.1. Characterization of Pickering emulsion

TiO₂ nanoparticles are of suitable hydrophilicity and could be used as the stabilizer of oil-in-water emulsion. Fig. 1A and B presents the digital photographs of the Pickering emulsion stabilized with TiO₂ nanoparticles before and after violent shaking. It could be clearly found that the transparent oil phase, which consists of MAA, EGDMA, DBP, HD and AIBN, is located at the top of the tube reactor, while the aqueous dispersion of TiO₂ nanoparticles is located at the bottom of tube reactor before violent shaking because of density difference. After violent shaking, the TiO₂ nanoparticles are attached to the droplet surface and a milk-like emulsion is obtained as shown in Fig. 1B. It is worth mentioning that the obtained Pickering emulsion is enough stable without the rising or sinking of emulsion droplets during the observation period.

In order to observe the morphology and size of Pickering emulsion droplets stabilized with TiO₂ nanoparticles, the optical microscope characterization was performed, and the photographs are shown in Fig. 2. It is displayed clearly that the Pickering emulsion droplets of H-MIPs and H-NIPs both appear broad size distribution, and there is no marked difference in shape and size, which indi-



Fig. 1. Digital photographs of the Pickering emulsion stabilized with TiO₂ nanoparticles before (A) and after (B) violent shaking.

cates that the addition of DBP has no remarkable influence on the morphology of Pickering emulsion droplets. The two types of emulsion droplets both show a regular spherical morphology with different sizes of emulsion droplets coexisting simultaneously. The diameters of emulsion droplets vary from 20 to 100 μm.

3.2. Characterization of H-MIPs microspheres

After thermal initiation, the free radical polymerization would proceed within the Pickering emulsion droplets, and the H-MIPs and H-NIPs microspheres could be obtained after a series of post-treatment procedure. The H-MIPs and H-NIPs microspheres were both observed by optical microscope, and the photographs are shown in Fig. 3. It is obvious that the morphology of H-MIPs and H-NIPs microspheres has no significant difference and both appear irregular spherical shape with slight sunken surfaces because of the presence of HD during the polymerization process, which is a nonreactive solvent and does not participate in the polymerization. The more refined surface features of H-MIPs and H-NIPs microspheres could be not distinguished because of the limited resolution of the optical microscope. Thus, H-MIPs and H-NIPs microspheres need to be characterized further by FESEM because of its higher resolution.

TiO₂ nanoparticles were observed by FESEM to obtain their morphology and the corresponding FESEM image is shown in Fig. 4. It could be found that the TiO₂ nanoparticles are of spherical form with narrow size distribution, and the average size of TiO₂ nanoparticles is about 20 nm.

The FESEM images of H-MIPs and H-NIPs microspheres are exhibited in Fig. 5. It is clear that the morphology of H-MIPs and H-NIPs microspheres has no significant difference, implying that

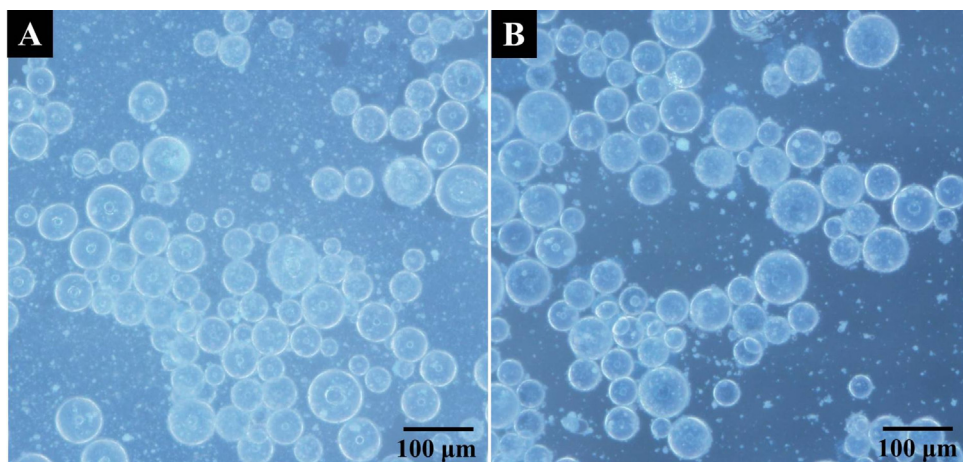


Fig. 2. Optical microscope photographs of Pickering emulsion droplets stabilized with TiO_2 nanoparticles (A: H-MIPs; B: H-NIPs).

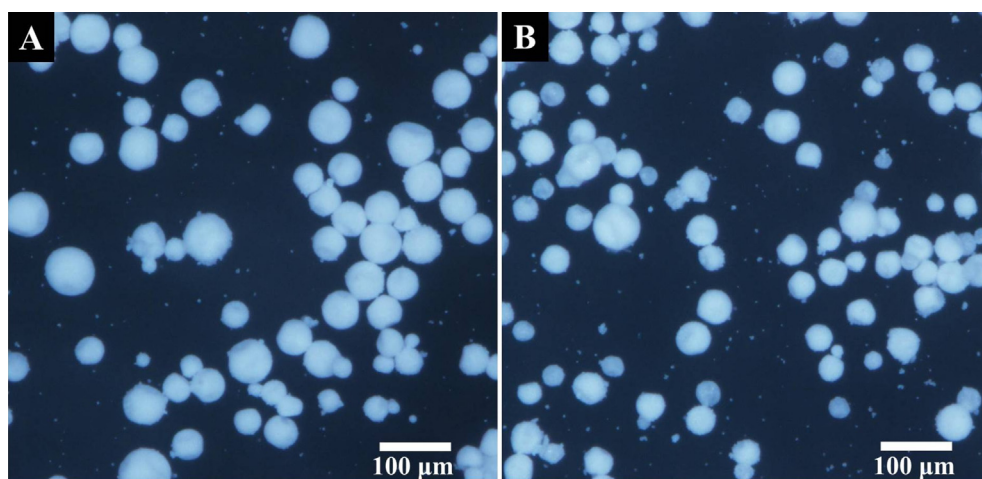


Fig. 3. Optical microscope photographs of H-MIPs (A) and H-NIPs (B) microspheres.

the addition of DBP has no influence on the morphology of microspheres. These microspheres are of a wide size distribution and appear irregular spherical shape with one to three sunken on the surface. The appearance of sunken surface originates from the shrinkage of Pickering emulsion droplets during the polymerization with high temperature and indicates that the interior of polymer microspheres is not solid but hollow (Qin et al., 2020). The formation of hollow structure results from the polymerization induced phase separation within the droplets of Pickering emulsion. It is well-known that HD is the poor solvent for the resulting copolymer. When the polymerization is initiated, the interfacial tension would force the copolymer phase to migrate towards the interface to form the polymer shell and the HD remains in the center of emulsion droplets (Chen et al., 2007; Zhang et al., 2014). Due to the fluidity of HD, the collapse of polymer shell layer may occur random during the polymerization process. When HD is removed by washing, the hollow structure is formed finally. Fig. 5C presents the FESEM image of a single H-MIPs microsphere under high magnification. Two sunken surfaces could be clearly seen on the microspheres, which are formed during the polymerization and imply the presence of hollow structure. Besides, TiO_2 nanoparticles located on the surface of microsphere are also recognized, which packed polymer microspheres tightly. Fig. 5D shows the internal structure of a broken H-MIPs microsphere. It is shown clearly that H-MIPs microspheres are of perfect hollow structure, which is consistent with the above judgment.

Additionally, the size distribution of H-MIPs and H-NIPs microspheres could be obtained accurately from the FESEM images under a relative low magnification, which contain much more microspheres in the field of view. The corresponding FESEM images are displayed in supporting information as Fig. S1. The size distribution frequency of H-MIPs and H-NIPs microspheres is obtained

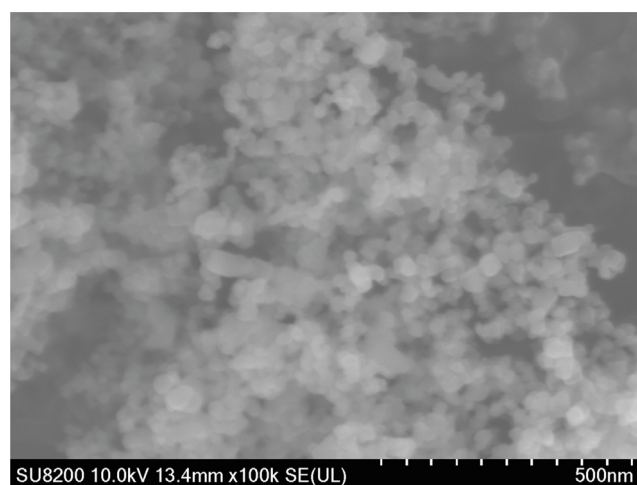


Fig. 4. FESEM image of TiO_2 nanoparticles.

separately by counting 150 microspheres using Nano Measurer 1.2 software, and the results are shown in Fig. 6. It could be found that H-MIPs microspheres appear broad size distribution, whose sizes vary from 20 to 100 μm and the mean size is about 43 μm . The size of H-NIPs microspheres range from 18 to 70 μm and the average size is approximately 39 μm . The difference of size distribution frequency between H-MIPs and H-NIPs derives from the region selection during FESEM characterization.

The chemical structures of H-MIPs and H-NIPs microspheres were characterized by FTIR. The spectra are displayed in Fig. 7. The characteristic peaks at 1730 cm^{-1} , 1253 cm^{-1} and 1159 cm^{-1} are attributed to the C = O stretching vibration, C-O symmetric and asymmetric stretching vibrations of O = C-O groups, respectively. Meanwhile, the peak at 3618 cm^{-1} could be assigned to the stretching vibration of O-H from MAA. The appearance of these characteristic peaks indicates that MAA could polymerize with EGDMA by Pickering emulsion polymerization stabilized with TiO_2 nanoparticles. In addition, it is clearly pre-

sented that the spectra of H-MIPs and H-NIPs microspheres have no significant difference, which illustrates that the template of DBP has been removed completely from H-MIPs microspheres.

The thermal stability of H-MIPs and H-NIPs microspheres were further analyzed using TGA and the results are shown in Fig. 8. It is obvious that the two curves have no distinct difference. There is a fast weight loss due to the significant decomposition of the polymers when the temperature is above $230\text{ }^\circ\text{C}$. The final weight loss of H-MIPs (93.3%) could be observed when the temperature increases to $450\text{ }^\circ\text{C}$. There is no obvious change when the temperature further increases. The remaining mass is attributed to the TiO_2 nanoparticles, which serve as Pickering emulsion stabilizer and remain on the surface of the H-MIPs and H-NIPs microspheres.

3.3. Binding kinetics and isotherm

In order to accelerate mass transfer and improve the binding rate, we designed and prepared the H-MIPs microspheres. The

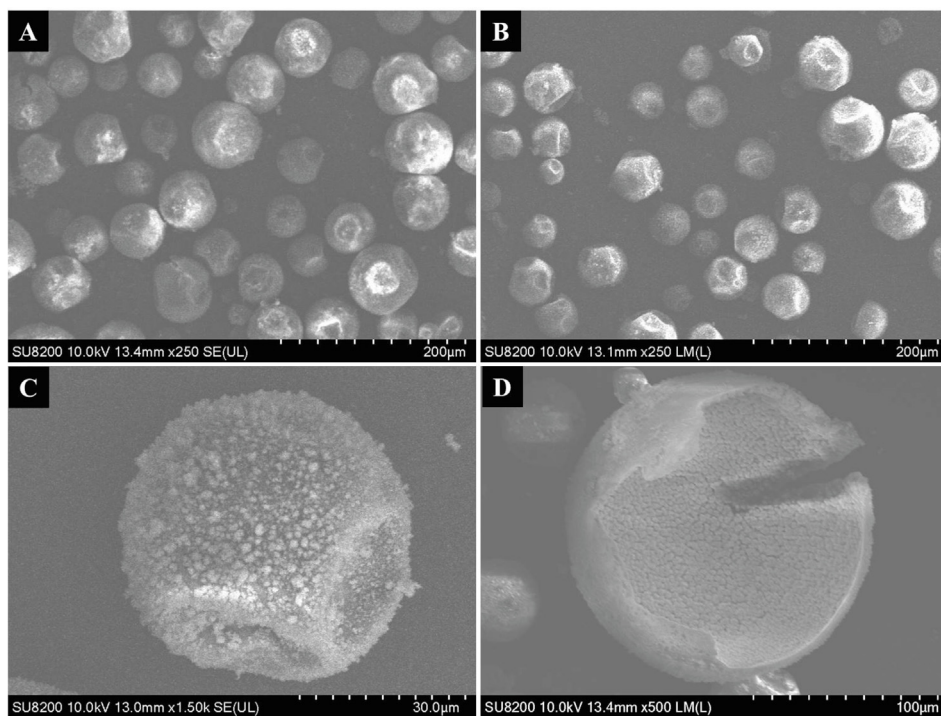


Fig. 5. FESEM images of H-MIPs (A) and H-NIPs (B) microspheres, single H-MIPs microsphere under high magnification (C) and the cross-section FESEM of broken H-MIPs microsphere.

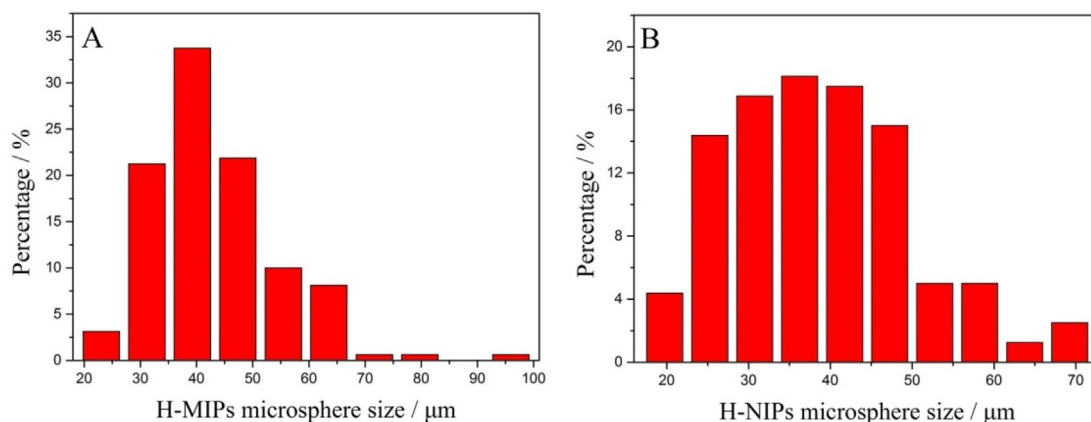


Fig. 6. The size distribution frequency of H-MIPs (A) and H-NIPs (B) microspheres.

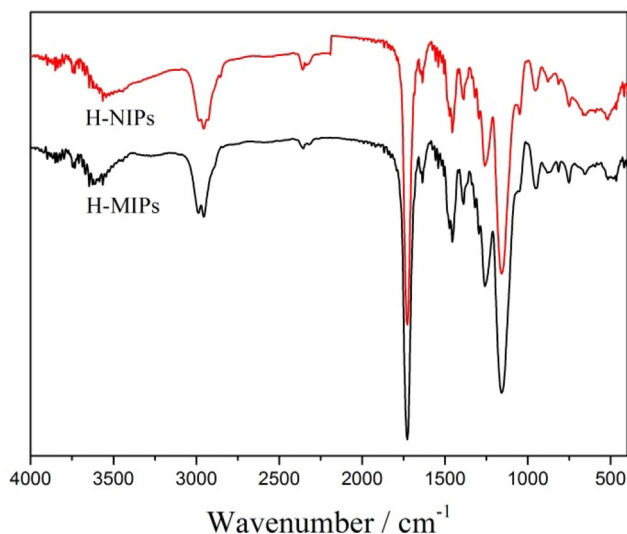


Fig. 7. FTIR spectra of H-MIPs and H-NIPs microspheres.

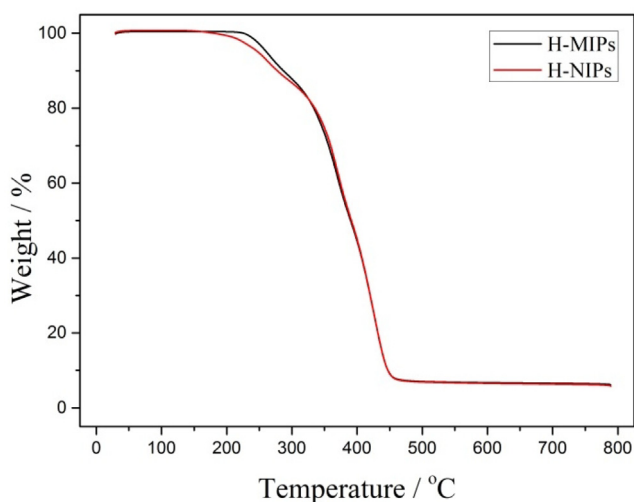


Fig. 8. TGA curves of H-MIPs and H-NIPs microspheres.

binding kinetics experiment was carried out in 1.0 mmol/L of DBP ethanol solution, and the result is displayed in Fig. 9. It could be found clearly that the binding amounts of H-MIPs and H-NIPs are closely related to time. The binding curves of H-MIPs and H-NIPs both appear three stages during the whole binding process. Firstly, the external binding sites quickly bind DBP because of small mass transfer resistance. Secondly, DBP begins to combine with interior binding sites, and the binding rate slows down with the increasing mass transfer resistance. Thirdly, the binding reaches saturation and the binding amounts do not change with the extension of time.

Table 1
Kinetic parameters of template binding on H-MIPs and H-NIPs via two kinetic models.

Sorbent	$B_{e,e}^a$ ($\mu\text{mol/g}$)	Pseudo-first-order equation			Pseudo-second-order equation		
		R^2	$B_{e,c}^b$ ($\mu\text{mol/g}$)	k_1^c (min^{-1})	R^2	$B_{e,c}^b$ ($\mu\text{mol/g}$)	k_2^d ($\text{g } \mu\text{mol}^{-1} \text{min}^{-1}$)
H-MIPs	128.0	0.9921	127.8	0.1769	0.9865	135.8	0.2297×10^{-2}
H-NIPs	50.05	0.9996	50.04	0.1790	0.9878	53.19	0.5851×10^{-2}

^a $B_{e,e}$ is the experimental value of B_e .

^b $B_{e,c}$ is the calculated value of B_e .

^c k_1 is the rate constant of first-order adsorption.

^d k_2 is the rate constant of second-order adsorption.

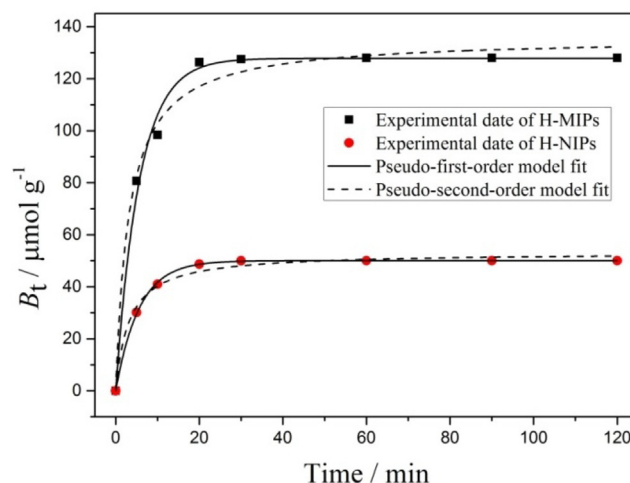


Fig. 9. Binding kinetics data and modeling for the binding of DBP on H-MIPs and H-NIPs microspheres.

The binding saturation of H-MIPs and H-NIPs microspheres could be reached within 30 min, which results from the low mass transfer resistance because of the presence of hollow structure. Additionally, we found that the binding amounts of H-MIPs are all higher than that of H-NIPs at each test time point, which results from the presence of imprinted sites with higher affinity towards DBP and indicates that the imprinted sites have been successfully constructed on the H-MIPs microspheres.

Besides, the binding kinetic data of H-MIPs and H-NIPs were both fitted through pseudo-first-order and pseudo-second-order kinetic model to elucidate the potential rate-controlling step. The fitting curves are also shown in Fig. 9, and all calculated results and the values of R^2 are listed in Table 1. It could be found clearly that the pseudo-first-order model fits all the binding data better than the pseudo-second-order model, which is judged by the higher correlation coefficients and suggests that the physical interactions are possibly involved in the binding process, and the binding rate is controlled by the diffusion of template molecules within the material.

Aside from the binding kinetics, the binding equilibrium experiment was also performed. Fig. 10 displays the binding amounts of DBP on the H-MIPs and H-NIPs microspheres under different initial concentrations. It could be seen clearly that the DBP bound by H-MIPs and H-NIPs both increases with the increasing initial DBP concentration from 0.5 to 3.0 mmol/L. Furthermore, the H-MIPs microspheres could bind much more DBP than H-NIPs microspheres over the whole tested concentration range. The distinction of the binding amounts between H-MIPs and H-NIPs increases with the increasing DBP initial concentration. These results suggest that the H-MIPs microspheres are of much higher affinity towards DBP than H-NIPs microspheres because of the imprinting effect, verifying the advantage of the building of the imprinted sites.

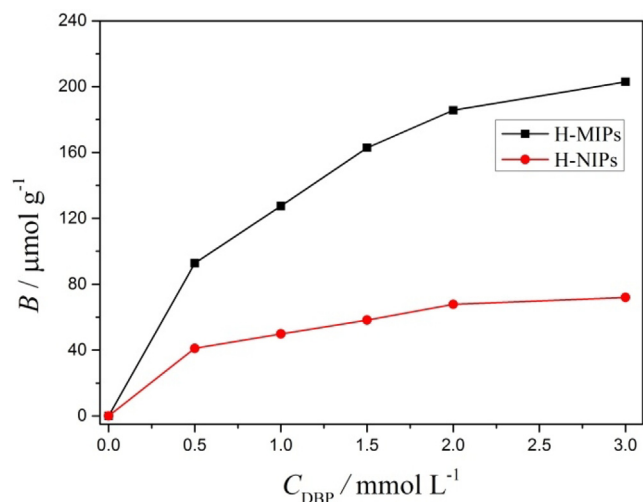


Fig. 10. Binding isotherms of H-MIPs and H-NIPs microspheres.

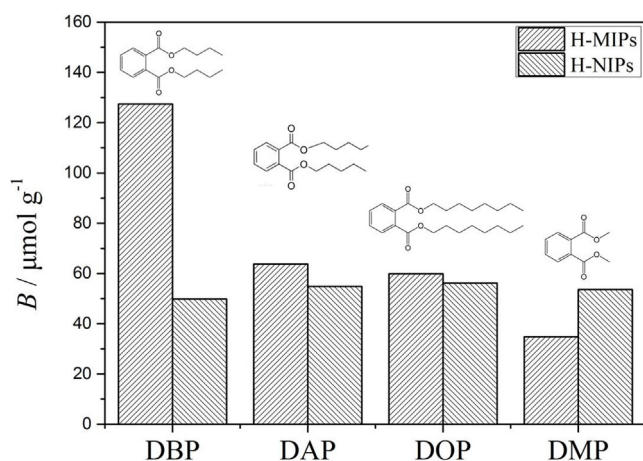


Fig. 11. The binding amounts of DBP, DAP, DOP and DMP on H-MIPs and H-NIPs microspheres.

3.4. Selectivity of H-MIPs microspheres

Selective experiment was performed to evaluate the binding specificity of H-MIPs microspheres towards DBP. The three compounds, DAP, DOP and DMP, were selected as controls in this experiment because of their structural similarity to DBP. Fig. 11 presents the binding amounts of H-MIPs and H-NIPs towards DBP, DAP, DOP and DMP, respectively. It could be found that the H-MIPs microspheres exhibit higher selectivity towards DBP than DAP, DOP and DMP. The imprinting factor could be obtained by the ratio of the binding amounts between H-MIPs and H-NIPs. The imprinting factors of H-MIPs towards DBP, DAP, DOP and DMP are found to be 2.56, 1.16, 1.06 and 0.65, respectively. The results indicate that the H-MIPs microspheres are of excellent selectivity towards the target molecules.

3.5. Reusability of H-MIPs microspheres

To evaluate the regeneration performance of obtained H-MIPs and H-NIPs microspheres, the sorption-desorption cycle was carried out repeatedly for 5 times. The experimental results are shown in Fig. 12. It could be found that the binding amount of H-MIPs microspheres towards DBP remains at a high level within 3 cycles.

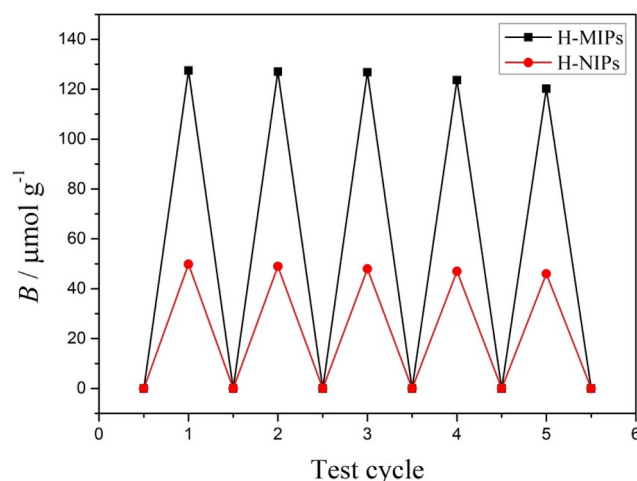


Fig. 12. The binding amounts of H-MIPs and H-NIPs microspheres in different rebinding cycles.

There is no significant decrease in the binding amount during the first 3 cycles. After 3 cycles, the binding amount witnesses a downward trend, but the reduced amount is limited. Therefore, the imprinted sites of H-MIPs are of certain stability and the H-MIPs microspheres could be reused after regeneration. In addition, it could be found that the binding amounts of H-NIPs microspheres show a gradually decreasing trend with the increase of test cycles.

4. Conclusions

H-MIPs microspheres towards DBP were synthesized via facile Pickering emulsion polymerization stabilized with TiO₂ nanoparticles. Nonreactive HD plays a critical role during the polymerization induced phase separation. The hollow structure was confirmed by optical microscope and FESEM observation. The synthetic method does not require the calcination or etching process, which are indispensable in traditional construction of hollow structure. The H-MIPs show excellent binding kinetics and could reach binding equilibrium within 30 min. Additionally, H-MIPs also show accurate selectivity towards DBP with the imprinting factor of 2.56, which is larger than that of DAP, DOP and DMP. Furthermore, the imprinted sites of H-MIPs are of certain stability and the H-MIPs microspheres could be reused after regeneration within the limited cycles. These results show that H-MIPs microspheres are promising adsorbents in terms of environmental protection. Meanwhile, the study also provides an optional method for the facile fabrication of H-MIPs microspheres.

CRediT authorship contribution statement

Zehu Wang: Writing – original draft. **Zongqi Li:** Visualization, Investigation. **Ruiye Yan:** Methodology, Software. **Guangshuo Wang:** Conceptualization. **Yanming Wang:** Data curation. **Xiaoliang Zhang:** Supervision, Validation. **Zhixiao Zhang:** Writing – review & editing.

Declaration of Competing Interest

The authors declare that they have no known competing financial interests or personal relationships that could have appeared to influence the work reported in this paper.

Acknowledgments

This work was funded by the Science and Technology Project of Hebei Education Department (Grant No. QN2021036), the Natural Science Foundation of Hebei Province (Grant No. E2021402004), and the Central Government Guides Local Science and Technology Development Fund (216Z1202G, 206Z1201G).

Appendix A. Supplementary material

Supplementary data to this article can be found online at <https://doi.org/10.1016/j.arabjc.2023.105304>.

References

- Bayramoglu, G. et al., 2016. Removal of bisphenol A from aqueous medium using molecularly surface imprinted microbeads. *Chemosphere* 150, 275–284.
- BelBruno, J.J. et al., 2019. Molecularly imprinted polymers. *Chem. Rev.* 119, 94–119.
- Belkhanchi, H. et al., 2020. Synthesis of N-CNT/TiO₂ composites thin films: surface analysis and optoelectronic properties. *E3S Web Conf.* 183, 05002.
- Belkhanchi, H. et al., 2021. Nitrogen doped carbon nanotubes grafted TiO₂ rutile nanofilms: Promising material for dye sensitized solar cell application. *Optik* 229, 166234.
- Chen, T. et al., 2007. Organic-inorganic hybrid hollow spheres prepared from TiO₂-stabilized Pickering emulsion polymerization. *Adv. Mater.* 19, 2286–2289.
- Dharma, H. et al., 2022. A review of titanium dioxide (TiO₂)-based photocatalyst for oilfield-produced water treatment. *Membranes* 12, 345.
- Eidsvg, H. et al., 2021. TiO₂ as a photocatalyst for water splitting—an experimental and theoretical review. *Molecules* 26, 1687.
- Gao, R. et al., 2016. A highly-efficient imprinted magnetic nanoparticle for selective separation and detection of 17 β -estradiol in milk. *Food Chem.* 194, 1040–1047.
- Guo, H. et al., 2018. Surface molecular imprinting on carbon microspheres for fast and selective adsorption of perfluorooctane sulfonate. *J. Hazard. Mater.* 348, 29–38.
- He, S. et al., 2021. Advances of molecularly imprinted polymers (MIP) and the application in drug delivery. *Eur. Polym. J.* 143, 110179.
- Htwe, A.T. et al., 2022. Synthesis of chitosan-coated magnetite nanoparticles using coprecipitation method for copper (II) ions removal in aqueous solution. *World J. Eng.* 19, 726–734.
- Jena, H. et al., 2021. The effect of clam shell powder on kinetics of water absorption of jute epoxy composite. *World J. Eng.* 18, 684–691.
- Jia, Y. et al., 2021. Facile synthesis of molecularly imprinted black TiO₂-x/carbon dots nanocomposite and its recognizable photocatalytic performance under visible-light. *Appl. Surf. Sci.* 551, 149476.
- Karsten, P.X. et al., 2020. Molecularly imprinted polymers: antibody mimics for bioimaging and therapy. *Chem. Rev.* 120, 9554–9582.
- Kubo, A. et al., 2021. Enantioseparation of warfarin derivatives on molecularly imprinted polymers for (S)- and (R)-chlorowarfarin. *J. Chromatogr. A* 1641, 461995.
- Liu, X. et al., 2019. Synthesis of molecularly imprinted polymer by suspension polymerization for selective extraction of p-hydroxybenzoic acid from water. *J. Appl. Polym. Sci.* 136, 46984–46992.
- Luo, J. et al., 2022. A mesoporous silica-based probe with a molecularly imprinted polymer recognition and Mn:ZnS QDs@rhodamine B ratiometric fluorescence sensing strategy for the analysis of 4-nitrophenol. *Anal. Methods* 14, 3881–3889.
- Mahajan, M.R. et al., 2019. Highly efficient synthesis and assay of protein-imprinted nanogels by using magnetic templates. *Angew. Chem. Int. Ed.* 58, 727–730.
- Min, G.C. et al., 2021. Characterization of hydrogel type molecularly imprinted polymer for creatinine prepared by precipitation polymerization. *Polymer* 237, 124348–124360.
- Mokhtari, P. et al., 2019. Water compatible molecularly imprinted polymer for controlled release of riboflavin as drug delivery system. *Eur. Polym. J.* 118, 614–618.
- Monllorsatoca, D. et al., 2021. Comparative photo-electrochemical and photocatalytic studies with nanosized TiO₂ photocatalysts towards organic pollutants oxidation. *Catalysts* 11, 349.
- Nguyen, T.B. et al., 2019. Photocatalytic degradation of bisphenol A over a ZnFe₂O₄/TiO₂ nanocomposite under visible light. *Sci. Total Environ.* 646, 745–756.
- Pan, J. et al., 2014. Magnetic molecularly imprinted microcapsules derived from Pickering emulsion polymerization and their novel adsorption characteristics for l-cyhalothrin. *RSC Adv.* 4, 4435–4443.
- Pickering, S.U., 1907. CXCVI-emulsions. *J. Chem. Soc. Transact.* 91, 2001–2021.
- Qin, Y.T. et al., 2020. Tumor-sensitive biodegradable nanoparticles of molecularly imprinted polymer-stabilized fluorescent zeolitic imidazolate framework-8 for targeted imaging and drug delivery. *ACS Appl. Mater. Interfaces* 12, 24585–24598.
- Roberto, A.D.M. et al., 2019. Selective photodegradation of 2,4-D pesticide from water by molecularly imprinted TiO₂. *J. Photoch. Photobio. A* 380, 111872–111877.
- Schrade, A. et al., 2013. Pickering-type stabilized nanoparticles by heterophase polymerization. *Chem. Soc. Rev.* 42, 6823–6839.
- Shen, X. et al., 2011. Interfacial molecular imprinting in nanoparticle-stabilized emulsions. *Macromolecules* 44, 5631–5637.
- Sun, P. et al., 2020. Controllable synthesis of TiO₂: toward an efficient photocatalyst. *New Horiz. Photocatal.* 39–55.
- Tian, H.S. et al., 2020. Hydrophilic magnetic molecularly imprinted nanobeads for efficient enrichment and high performance liquid chromatographic detection of 17 β -estradiol in environmental water samples. *Talanta* 220, 121367–121375.
- Wang, Z. et al., 2018. Polymerization induced shaping of Pickering emulsion droplets: from simple hollow microspheres to molecularly imprinted multicore microrattles. *Chem. Eng. J.* 332, 409–418.
- Wang, Z. et al., 2018. The synthesis of molecular recognition polymer particles via miniemulsion polymerization. *React. Funct. Polym.* 126, 1–8.
- Wulff, G. et al., 2013. Fourty years of molecular imprinting in synthetic polymers: origin, features and perspectives. *Microchim. Acta* 180, 1359–1370.
- Xu, W.Z. et al., 2011. A molecularly imprinted polymer based on TiO₂ as a sacrificial support for selective recognition of dibenzothiophene. *Chem. Eng. J.* 172, 191–198.
- Zarhri, Z. et al., 2020. Synthesis, structural and crystal size effect on the optical properties of sprayed TiO₂ thin films: Experiment and DFT TB-mbj. *J. Alloy. Compd.* 819, 153010.
- Zhang, Y. et al., 2014. A facile route toward structured hybrid particles based on liquid-solid assembly. *Macromolecules* 47, 1030–1038.
- Zhang, Y. et al., 2014. Encapsulated phase change materials stabilized by modified graphene oxide. *J. Mater. Chem. A* 2, 5304–5314.
- Zhang, K. et al., 2019. Chromatographic separation of hemoglobin variants using robust molecularly imprinted polymers. *Talanta* 199, 27–31.
- Zhang, L.P.W. et al., 2020. Preparation, characterization, and application of soluble liquid crystalline molecularly imprinted polymer in electrochemical sensor. *Anal. Bioanal. Chem.* 412, 7321–7332.
- Ziat, Y. et al., 2022. CNTs modified ZnO and TiO₂ thin films: The effect of loading rate on band offset at metal/semiconductor interfaces. *E3S Web Conf.* 337, 05003.